

Bluecat: A Local Uncertainty Estimator for Deterministic Simulations and Predictions

D. Koutsoyiannis¹, and A. Montanari²

¹National Technical University of Athens, Zographou, Greece

²Department DICAM, University of Bologna, Bologna, Italy

Key Points:

- We propose a new method to frame a deterministic prediction model into a stochastic setting with probability based uncertainty assessment.
- We theoretically and empirically prove the optimal performance of the method for operational applications.
- We provide an open source computer code to apply the method and perform diagnostic checking.

Corresponding author: Alberto Montanari, alberto.montanari@unibo.it

Abstract

We present a new method for simulating and predicting hydrologic variables with uncertainty assessment and provide example applications to river flows. The method is identified with the acronym “Bluecat” and is based on the use of a deterministic model which is subsequently converted to a stochastic formulation. The latter provides an adjustment on statistical basis of the deterministic prediction along with its confidence limits. The distinguishing features of the proposed approach are the ability to infer the probability distribution of the prediction without requiring strong hypotheses on the statistical characterization of the prediction error (e.g. normality, homoscedasticity) and its transparent and intuitive use of the observations. Bluecat makes use of a rigorous theory to estimate the probability distribution of the predictand conditioned by the deterministic model output, by inferring the conditional statistics of observations. Therefore Bluecat bridges the gaps between deterministic (possibly physically-based, or deep learning-based) and stochastic models as well as between rigorous theory and transparent use of data with an innovative and user oriented approach. We present two examples of application to the case studies of the Arno river at Subbiano and Sieve river at Fornacina. The results confirm the distinguishing features of the method along with its technical soundness. We provide an open software working in the R environment, along with help facilities and detailed instructions to reproduce the case studies presented here.

Plain Language Summary

We present a new method for simulating and predicting hydrologic variables and in particular river flows, which is rooted in the probability theory and conceived in order to provide a reliable quantification of its uncertainty for operational applications. In fact, recent practical experience during extreme events has shown that simulation and prediction uncertainty is essential information for decision makers and the public. A reliable and transparent uncertainty assessment has also been shown to be essential to gain public and institutional trust in real science. Our approach, which we term with the acronym “Bluecat”, results from a theoretical and numerical development, and is conceived to make a transparent and intuitive use of the observations which in turn mirror the observed reality. Therefore, Bluecat makes use of a rigorous theory while at the same time proofing the concept that environmental resources should be managed by making the best use of empirical evidence and experience. We provide an open and user friendly software to apply the method to the simulation and prediction of river flows and test Bluecat’s reliability for operational applications.

1 Introduction

Recent extreme events like the flood that occurred in central Europe in 2021 have shown that reliable hydrological predictions are essential to issue early warnings to institutions and population. Indeed, effective warnings require people to be informed on the magnitude of a forthcoming event and the likelihood of that happening. Namely, a prediction along with its uncertainty needs to be timely developed and communicated. The time factor is in fact essential and therefore the whole warning system needs to be fast and reliable, in the estimation of both prediction and uncertainty (see, for instance, Ramos et al. (2013) and Pagano et al. (2014)). An additional key element for the success of a warning system is its credibility, which is usually evaluated by end users by confronting the prediction method with their expert judgment and empirical evaluation (Blöschl, 2008). This is precisely the reason why the prediction and its uncertainty should be elaborated with a transparent approach by making a perceptual use of the available information and data, which in turn mirror the observed reality of previous and likely future events.

62 In particular, the uncertainty inherent in scientific information is one of the rea-
63 sons for failing to act on disaster warnings. Forecasts are often elaborated with method-
64 ologies that are not easily understood by those who need it. Such lack of understand-
65 ing of uncertainty estimation may lead people to interpret the predictions as unreliable,
66 and to believe that estimations should no longer be trusted.

67 Prediction and forecasting have been the focus of an intensive research activity in
68 hydrology (see, for instance, Blöschl et al. (2013)). Here, we concentrate on uncertainty
69 assessment which has been the subject of relevant efforts since the early works of Spear
70 and Hornberger (1980) and Beven and Binley (1992). The literature is branched in sev-
71 eral subtopics ranging from data uncertainty, parameter fitting, model structural uncer-
72 tainty, operational uncertainty and so forth (Montanari, 2011).

73 To date, the most used method for estimating the uncertainty of hydrological sim-
74 ulations and predictions is the Generalized Likelihood Uncertainty Estimator (GLUE)
75 (see Beven and Binley (1992) and Beven (2006)). GLUE rejects the concept of one sin-
76 gular optimal model and adopts the notion of equifinality of modeling solutions (Beven &
77 Lane, 2019). It makes use of an informal likelihood function that has been the subject
78 of an interesting debate (see, for instance, Montanari (2005); Vrugt et al. (2009); Beven
79 (2009)). Bayesian methods are widely used and include, among the others, Bayesian model
80 averaging (see the recent work by Reggiani et al. (2021)), Bayesian estimation of model
81 errors (Tajiki et al., 2020) and Bayesian data assimilation (Bulygina & Gupta, 2009),
82 and signature domain calibration (Kavetski et al., 2018). In a Bayesian framework, iden-
83 tifying a suitable likelihood function for hydrological models is a challenging task which
84 requires the introduction of assumptions that need to be carefully checked as sometimes
85 the related approximations are not easily understandable by end users.

86 Another relevant example of Bayesian method is the Bayesian Forecasting System
87 introduced by Krzysztofowicz (1999), which produces a probabilistic river stage or flow
88 forecast based on a probabilistic quantitative precipitation forecast as an input to a hy-
89 drological model. The BFS assumes that the dominant source of uncertainty derives from
90 the imperfect knowledge of the future precipitation, so that it can be assumed that all
91 other sources of uncertainty play a minor role. While it may be justified for operational
92 forecasting, this assumption looks restrictive for hydrologic simulations where model struc-
93 tural uncertainty may also be substantial.

94 The literature presented several approaches to uncertainty assessment based on the
95 statistical analysis of the probability distribution of model errors or, analogously, the joint
96 probability distribution of observed and simulated data. These methods belong to the
97 category of the post-processing approaches, which have been proved to outperform anal-
98 yses that consider all the sources of uncertainty (see, for instance, the recent contribu-
99 tion by Valdez et al. (2021)). This class of methods can be further subdivided in like-
100 lihood based and likelihood-free approaches. The use of likelihood is considered by Tajiki
101 et al. (2020) and previously by Schoups and Vrugt (2010), while likelihood-free meth-
102 ods include the works by Montanari and Brath (2004), Montanari and Grossi (2008) and
103 Montanari and Koutsoyiannis (2012). The statistical analysis of model errors to estimate
104 simulation and prediction uncertainty with a likelihood-free approach presents the ad-
105 vantage of being transparent to end users and computationally fast.

106 In particular, Montanari and Koutsoyiannis (2012) proposed a theoretically based
107 method to convert a deterministic hydrologic model into a stochastic approach by fit-
108 ting the model error with a meta-Gaussian probability distribution. A similar approach
109 was applied by Quilty and Adamowski (2020) and several other works. Notably, Sikorska
110 et al. (2015) proposed a nearest neighbour approach to represent the probability distri-
111 bution of the model error which makes the method flexible and fast. Similar approaches
112 were applied by Papacharalampous, Tyralis, and Koutsoyiannis (2019), Papacharalampous
113 et al. (2020), Papacharalampous, Tyralis, Langousis, et al. (2019b), Tyralis, Papachar-

114 alampous, and Langousis (2019), Tyralis, Papacharalampous, Burnetas, and Langousis
 115 (2019) and Papacharalampous, Tyralis, Langousis, et al. (2019a). Notwithstanding the
 116 above research efforts, the statistical representation of the model error remains difficult
 117 in some applications and thus there is still the need for end users to further simplify the
 118 procedure.

119 In view of the above previous works and the requirement for effective predictions,
 120 we present here an innovative and transparent approach that builds on the concept pro-
 121 posed by Montanari and Koutsoyiannis (2012) to transform a generic deterministic model
 122 into a stochastic predictor. A distinguishing feature of the proposed method is its abil-
 123 ity to infer the probability distribution of the prediction without running multiple sim-
 124 ulations and without requiring strong hypotheses on the statistical characterization of
 125 the prediction itself or its error, therefore resolving critical issues that affect the previ-
 126 ously proposed methods. Although intuitive, the method is supported by a rigorous theo-
 127 retical development that ensures the best use of the information content of the observed
 128 data. The method can be applied to either physically-based, process-based and data-based
 129 deterministic prediction/simulation models. It can also be applied in conjunction with
 130 prediction models based on deep learning, which are gaining increasing popularity for
 131 hydrological predictions (see, for instance, Frame et al. (2021)).

132 We make available an open software in the public domain, working in the R en-
 133 vironment (R Core Team, 2013), along with instructions and examples of applications,
 134 to support applications by end users. The software also provides goodness of fit proce-
 135 dures that are based on the best practices of engineering and applied forecasting.

136 We propose for our approach the acronym Bluecat, from “**B**risk local **u**ncertainty
 137 **e**stimator for generic **s**imulations and **p**redictions”. In this paper we focus on river flow
 138 and therefore assume that the deterministic model is a rainfall-runoff model. However,
 139 the procedure can be generalized to any type of deterministic prediction model. In what
 140 follows, we use the term “prediction” to encompass simulation, prediction and forecast-
 141 ing.

142 2 Concept of Bluecat

143 Bluecat is a simple and transparent tool to transform point predictions obtained
 144 by any deterministic model in stochastic predictions, therefore deriving the probability
 145 distribution of the predictand. In what follows, we will use the terms “D-model” and “S-
 146 model” to denote the deterministic model and its stochastic counterpart, respectively.

147 The information that is needed to perform the above transformation is obtained
 148 in Bluecat by building on the well established concept of comparing the D-model out-
 149 put with observed data; namely, the same concept that we commonly use for parame-
 150 ter estimation. Basing on such comparison, Bluecat estimates the probability distribu-
 151 tion of observed data conditioned on the D-model output and therefore obtains the cor-
 152 responding S-model output, along with its mean (or median) value and confidence band.
 153 It is important to make clear that the S-model prediction may be markedly different from
 154 the D-model one. In fact, the latter is not necessarily included into the confidence band
 155 of the S-model, which are displaced around the mean prediction of the S-model itself.
 156 Such possible outcome is schematically represented in Figure 1, where the concept of Blue-
 157 cat is depicted.

158 Being based on the comparison between the D-model output and the observations,
 159 Bluecat is therefore transparent and easily understandable, while the theoretical devel-
 160 opment that we present in Section 3 ensures that such interpretation of uncertainty is
 161 rigorous and asymptotically consistent in estimating global uncertainty.

162 Bluecat is based on the following main assumptions:

- 163 1. A single D-model is considered, with a single parameter set. Section 6 will present
 164 a discussion on the possible extension of the Bluecat concept to multimodel ap-
 165 plications.
 166 2. The stochastic processes describing the modelled variables are stationary during
 167 the calibration and application period. Non-stationarity can be accounted for by
 168 using non-stationary D-models (Koutsoyiannis & Montanari, 2015; Montanari &
 169 Koutsoyiannis, 2014a). Such extension is not considered in the present contribu-
 170 tion but a discussion is provided in Section 6.
 171 3. The calibration data set is extended enough to ensure that sufficient information
 172 is available to upgrade the D-model into the S-model.

173 Further assumptions will be introduced and discussed in Section 3.

174 The third assumption above highlights that the S-model, like the D-model, needs
 175 a proper calibration, which implies that a sufficiently long record of observed data, re-
 176 ferring to a variety of hydrologic conditions, is available for model training. Such require-
 177 ment may be difficult to satisfy in real world applications, which often refer to poorly
 178 gauged or ungauged conditions. We will discuss in Section 6 the implications of running
 179 Bluecat with a limited training.

180 The flow chart of the procedure for applying Bluecat is as follows (see Figure 1):

- 181 1. The D-model is calibrated by using observed data;
 182 2. At the prediction time t^* the D-model is run to produce an estimated river flow
 183 $Q(t)$ at time t ;
 184 3. A set of size m_1+m_2+1 (see Section 3.1 for details) of predicted river flows from
 185 the calibration data set, including the one with the smallest difference from $Q(t)$
 186 plus m_1 lower and m_2 greater in magnitude of it, is extracted and the correspond-
 187 ing simulated river flows $q_i, i = 1, \dots, 2m + 1$ are identified;
 188 4. From the obtained sample of q_i the mean (or median) prediction and the confi-
 189 dence band for assigned confidence level from the S-model are estimated by us-
 190 ing one of the methods described in Section 3.

191 Thus, the S-model operates an adjustment of the D-model to compensate its inability
 192 to fully reproduce the observed reality. We develop and present in the following section
 193 a theory to prove the rigorousness of the concept and the ability of the S-model to asymp-
 194 totically represent the desired probability distribution of the predictand.

195 **3 Theory of Bluecat**

196 We consider a hydrologic D-model transforming inputs \mathbf{x}_τ (e.g. rainfall) at discrete
 197 time τ to deterministic outputs Q_τ (e.g. river discharge) by means of a relationship that
 198 takes the form

$$199 \quad Q_\tau = G(\mathbf{x}_\tau), \quad (1)$$

200 where \mathbf{x}_τ is a vector containing a number of consecutive input variables, or even a ma-
 201 trix consisting of several input variables (such as rainfall, evapotranspiration, perhaps
 202 river discharge in an upstream basin, and possibly others). The transformation function
 203 is generally complicated, also involving additional state variables (e.g. soil moisture). A
 204 model is never identical to reality and the observed output (the predictand) q_τ will be
 205 different from the model prediction Q_τ . In the present work we consider the HyMod rainfall-
 206 runoff model (Boyle, 2000) as D-model, which involves 5 parameters.

207 As mentioned above, Montanari and Koutsoyiannis (2012) proposed a framework
 208 to upgrade a deterministic model into a stochastic one, which provides the probability
 209 distribution of the predictand given the inputs and the deterministic model output, con-

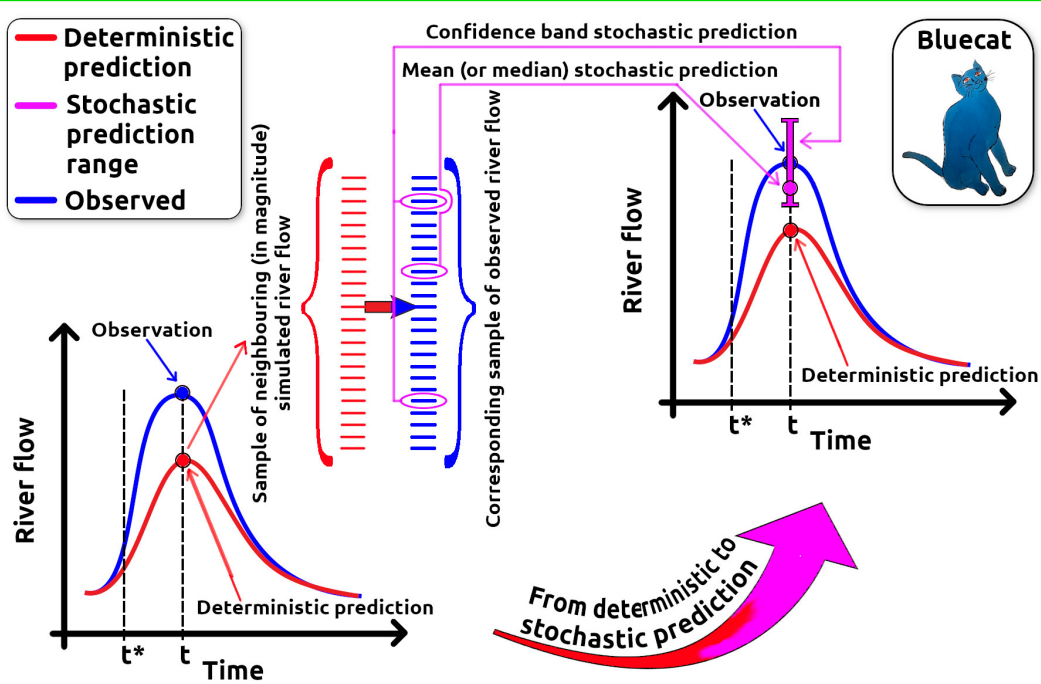


Figure 1. Schematic representation of the Bluecat concept underlying the transformation of the deterministic model (D-model) to a stochastic model (S-model). The painting in the upper right corner is cropped from the picture available at <https://www.flickr.com/photos/cizauskas/36142084534/> of the Andy Warhol exhibition at the High Museum, Atlanta, Georgia, USA (CC BY-NC-ND 4.0).

210 sidering the uncertainty in model parameters and input variables. This work has been
 211 discussed (Nearing, 2014; Montanari & Koutsoyiannis, 2014b) and advanced in other stud-
 212 ies (Sikorska et al., 2015; Quilty & Adamowski, 2020; Papacharalampous, Tyralis, & Kout-
 213 soyiannis, 2019). Here we pursue the same aim but in a different setting, with the pur-
 214 pose of upgrading the D-model into the S-model by using the simplest approach based
 215 on data analysis.

216 As anticipated in Section 2 we assume that the information contained in the true
 217 outputs q_τ and concurrent predictions by the D-model Q_τ is sufficient to support the above
 218 upgrade. This implies that the upgrade is properly trained over a sufficiently long cali-
 219 bration period. Transparency and ease of understanding of the procedure is a princi-
 220 pal objective and therefore we do not involve multiple simulations, but rather focus on
 221 a single model for which we aim to estimate the global prediction uncertainty. As a con-
 222 sequence, we do not consider parameter uncertainty in the D-model on the basis that
 223 another parameter set is in fact another model. This assumption is further discussed in
 224 Section 6.

225 Second, we do not subdivide uncertainty in different components as Bluecat au-
 226 tomatically incorporate all types, including the uncertainty in input data and param-
 227 eters, for which no particular provision is necessary. As already mentioned, the frame-
 228 work also assumes stationarity. If different subperiods are characterized by different model
 229 parameters or different input uncertainty, then one can split the entire simulated period
 230 in subperiods in which stationarity can be safely assumed. In alternative, the assump-
 231 tion of stationarity may be relaxed by considering a non-stationary D-model, as discussed
 232 in Section 6.

233 For advancing the D-model into its corresponding S-model we regard all related
 234 quantities as stochastic (random) variables and their sequences as stochastic processes.
 235 For notational clarity we underline stochastic variables, stochastic processes and stochas-
 236 tic functions. We use non-underlined symbols for non stochastic variables and determin-
 237 istic functions, as well as for realizations of stochastic variables and stochastic processes,
 238 where the latter realizations are also known as time series.

239 We assume that the inputs $\underline{\mathbf{x}}_\tau$, at discrete times τ , have a stationary probability
 240 density function $f_{\mathbf{x}}(\mathbf{x})$ and distribution function $F_{\mathbf{x}}(\mathbf{x})$. The output \underline{q}_τ depends on the
 241 inputs $\underline{\mathbf{x}}_\tau$ and is given through some stochastic function (S-model) as

$$242 \quad \underline{q}_\tau = g(\underline{\mathbf{x}}_\tau). \quad (2)$$

243 The stochastic process \underline{q}_τ is assumed to correspond to the real process, while the out-
 244 come of the deterministic model (D-model) of eq. (1) is an estimate thereof. By consid-
 245 ering \mathbf{x}_τ in eq. (1) as a stochastic process, retaining however the function $G(\neq g)$ as a
 246 deterministic function, we obtain the estimator \underline{Q}_τ of the output \underline{q}_τ as:

$$247 \quad \underline{Q}_\tau = G(\underline{\mathbf{x}}_\tau). \quad (3)$$

248 To advance from the D-model, in its form (3), to the S-model in (2) we just need
 249 to specify the conditional distribution:

$$250 \quad F_{q|Q}(q|Q) = P\{\underline{q} \leq q | \underline{Q} = Q\}, \quad (4)$$

251 with q and Q assumed concurrent and referring to discrete time τ . In other words, here
 252 conditioning is meant in scalar setting. An extension where Q is a vector containing the
 253 current and earlier predictions by the D-model and possibly other variables is straight-
 254 forward but not considered here (see also the discussion in Section 6).

255 It is relatively easy to infer from data the marginal distribution and density func-
 256 tions of the S-variable \underline{q} and D-predicted variable \underline{Q} . Therefore we may assume that $f_q(q)$

257 and $f_Q(Q)$ are known. Then the conditional density sought should obey

$$258 \int_{-\infty}^{\infty} f_{q|Q}(q|Q) dq = 1 \quad (5)$$

259 and

$$260 \int_{-\infty}^{\infty} f_{q|Q}(q|Q) f_Q(Q) dQ = f_q(q). \quad (6)$$

261 Eq. (5) is trivial. If we set $z = F_Q(Q)$ in (6), with $Q = F_Q^{-1}(z)$, so that $f_Q(Q)dQ = dz$, we obtain

$$263 \int_0^1 f_{q|Q}(q|F_Q^{-1}(z)) dz = f_q(q). \quad (7)$$

264 By integration one finds

$$265 \int_0^q \int_0^1 f_{q|Q}(a|F_Q^{-1}(z)) dz da = F_q(q), \quad (8)$$

266 and changing the order of the integrals we finally find

$$267 \int_0^1 F_{q|Q}(q|F_Q^{-1}(z)) dz = F_q(q). \quad (9)$$

268 At this stage, if one has time series of concurrent Q and q , each of size n , and if $Q_{(i:n)}$
 269 is the i th smallest value in the time series of Q and $q_{(j:n)}$ is the j th smallest value in the
 270 time series of q , then the approximations $F_Q(Q_i) \approx i/n$ and $F_q(q_j) \approx j/n$ can be used
 271 and thus one approximates $F_q(q)$ in (9) as

$$272 \frac{1}{n} \sum_{i=1}^n F_{q|Q}(q|Q_{(i:n)}) \approx F_q(q), \quad (10)$$

273 and, for $q = q_j$,

$$274 \frac{1}{n} \sum_{i=1}^n F_{q|Q}(q_{(j:n)}|Q_{(i:n)}) \approx \frac{j}{n}. \quad (11)$$

275 Hence,

$$276 B_j := \sum_{i=1}^n F_{q|Q}(q_{(j:n)}|Q_{(i:n)}) = j. \quad (12)$$

277 We can thus attempt to determine $F_{q|Q}$ by minimizing the quantity

$$278 A := \sum_{j=1}^n (B_j - j)^2 = \sum_{j=1}^n \left(\sum_{i=1}^n F_{q|Q}(q_{(j:n)}|Q_{(i:n)}) - j \right)^2, \quad (13)$$

279 therefore obtaining the desired conditional distribution which leads to the formulation
 280 of the S-model corresponding to the D-model.

281 3.1 Determining the conditional distribution

282 In real world applications the D-model will provide an uncertain and possibly bi-
 283 ased prediction. In such cases the S-model is applied by sampling from the conditional
 284 distribution $F_{q|Q}(q|Q)$ which incorporates both a shift of the prediction Q toward the
 285 real value q (bias correction) and the probabilistic assessment of the stochastic error (un-
 286 certainty assessment). A necessary preliminary step is the definition of the above con-
 287 ditional distribution as defined by eq. (4).

288 One strategy to tackle the problem is to use a parametric relationship for the func-
 289 tion $F_{q|Q}(q|Q)$ and determine its parameters by minimizing the quantity A in eq. (12).

290 A possibility would be to assume $F_{q|Q}(q|Q)$ to be a Pareto-Burr-Feller (PBF) distribu-
 291 tion (see Koutsoyiannis (2021)) with constant tail indices ξ and ζ and scale parameter
 292 varying with Q . A similar approach would be to assume a copula $C(F_q(q), F_Q(Q))$ and
 293 determine $F_{q|Q}(q|Q)$ as

$$294 \quad F_{q|Q}(q|Q) = \frac{F_{qQ}(q, Q)}{f_Q(Q)}, \quad (14)$$

295 with

$$296 \quad F_{q|Q}(q, Q) = C(F_q(q), F_Q(Q)). \quad (15)$$

297 While a parametric approach like the above is attractive from many aspects, here
 298 we propose a fully data based approach, i.e. we try to determine $F_{q|Q}(q|Q)$ from the data
 299 alone (see figure 1). As the variables of interest in hydrology are of continuous type, we
 300 may expect that each value Q_τ in the available time series appears only once. Thus we
 301 cannot form a sample of observed data for a particular value of Q . However, as a sim-
 302 ple approximation of $F_{q|Q}(q|Q)$, we can form a sample $\bar{q}_i, i = 1, \dots, (m_1 + m_2 + 1)$, of
 303 Q -neighbours based on:

$$304 \quad F_{q|Q}(q|Q) = P\{\underline{q} \leq q|Q = Q\} \approx P\{\underline{q} \leq q|Q - \Delta Q_1 \leq \underline{Q} \leq Q + \Delta Q_2\} \approx \\
 305 \approx P\{\underline{q} \leq q|F_Q(Q) - \Delta F_1 \leq F_Q(Q) \leq F_Q(Q) + \Delta F_2\} =: F_{q|Q}(q|Q, \Delta F_1, \Delta F_2), \quad (16)$$

306 where the increments ΔQ_i and ΔF_i can be chosen based on the requirement that the
 307 intervals below and above the value Q (or $F_Q(Q)$) contain appropriate numbers of data
 308 values, $m_1 := \Delta F_1 n$ and $m_2 := \Delta F_2 n$, respectively. The numbers m_1 and m_2 should
 309 not be too large, so that $F_Q(Q) \pm \Delta F_{1,2}$ be close to $F_Q(Q)$, nor too small, so that the
 310 probability

$$311 \quad P\{\underline{q} \leq q|(F_Q(Q) - m_1/n \leq F_Q(Q) \leq F_Q(Q) + m_2/n)\} \quad (17)$$

312 can be estimated from the sample of \bar{q}_i . From the above probability distribution one can
 313 easily estimate the mean value, or alternatively the median which may be more robust
 314 against outliers, which gives the S-model prediction. As for the confidence limits one pos-
 315 sibility is to compute empirical quantiles through order statistics. For example, one may
 316 choose $\Delta F_1 = \Delta F_2 = \Delta F$ and $m_1 = m_2 = m$. If one sets, say, $m_1 = m_2 = m = 20$,
 317 i.e. $m_1 + m_2 + 1 = 41$, the lowest and highest quantiles that can be empirically esti-
 318 mated would correspond to $1/41 \approx 2.5\%$ and $1 - 1/40 \approx 97.5\%$, respectively. Con-
 319 versely, for probabilities 2.5% and 97.5%, which correspond to a confidence level of 95%,
 320 we can empirically estimate the corresponding quantiles of q as the minimum and the
 321 maximum observed value, respectively, in the sample \bar{q}_i of $m_1 + m_2 + 1$ values.

322 One should note that a sample size of $m_1 + m_2 + 1$ may not be obtained for the
 323 extreme values of the simulation, for which a number m_1 of lower predictions and a num-
 324 ber m_2 of higher ones may not be available. In such cases the sample size need to be re-
 325 duced accordingly.

326 We point out that order statistics deliver quantile estimation for a limited set of
 327 probabilities that correspond to the frequency of data in the sample \bar{q}_i . Therefore the
 328 above approach cannot be used for estimating quantiles for arbitrary probabilities of the
 329 conditional distribution $F_{q|Q}(q|Q)$. When such need arises, for instance when perform-
 330 ing large ensemble simulations, a parametric relationship for $F_{q|Q}(q|Q)$ should be adopted
 331 and fitted as suggested above. Since here we do not use a parametric approach, we will
 332 handle this problem by the concept of K-moments discussed in section 3.2, noting though
 333 that even this cannot exceed some limits imposed by the subsample length ($m_1 + m_2 +$
 334 1).

335 3.2 Robust Estimation of Empirical Quantiles

336 The above empirical estimation of quantiles through order statistics is based on one
 337 data point only, as it identifies the single observation that is closer in frequency to the

338 probability that corresponds to the desired confidence level. A possible solution to in-
 339 crease the robustness of the estimation is offered by the recently introduced concept of
 340 knowable moments (K-moments, see Koutsyiannis (2019, 2021)) which gives an alter-
 341 native for empirical quantile evaluation that is more reliable than order statistics as it
 342 combines many data points in each estimate. Furthermore, K-moments offer unbiased
 343 estimates of distribution quantiles, while the order statistics enable unbiased estimates
 344 of the distribution function. The two estimates may differ substantially for heavy-tailed
 345 distributions.

346 The noncentral knowable moment (or noncentral K-moment) of order (p, q) of the
 347 random variable \underline{x} is defined as (Koutsyiannis, 2019)

$$348 \quad K'_{pq} := (p - q + 1)E \left[(F(\underline{x}))^{p-q} \underline{x}^q \right], \quad (18)$$

349 with $p \geq q$ and E indicating the expected value. A most interesting special case is $q =$
 350 1 . In fact, the noncentral knowable moment of order $(p, 1)$ is given by

$$351 \quad K'_p = pE \left[(F(\underline{x}))^{p-1} \underline{x} \right], \quad (19)$$

352 with $p \geq 1$. A basic property that connects the K-moments with expectations of max-
 353 ima is

$$354 \quad K'_p = E \left[\underline{x}_{(p)} \right] = E \left[\max(\underline{x}_1, \underline{x}_2, \dots, \underline{x}_p) \right]. \quad (20)$$

355 For expectations of minima another type of K-moments is defined, as described in Koutsyiannis
 356 (2021). Therefore, by definition K'_p represents the expected value of the maximum of p
 357 copies of \underline{x} and thus it is an estimate for the empirical quantile, which is computed by
 358 considering the whole data sample.

359 A key step in the above procedure is the estimation of two K-moment orders p_h
 360 and p_l , corresponding to the desired confidence level, for the upper and lower confidence
 361 limit, respectively. We illustrate here below the procedure for computing p_h and refer
 362 to Koutsyiannis (2021) for details on the computation of p_l .

363 First, let us introduce the Λ -coefficient of order p_h as

$$364 \quad \Lambda_{p_h} := \frac{1}{p_h (1 - F(K'_{p_h}))}. \quad (21)$$

365 Λ_{p_h} varies only slightly with p_h . Any symmetric distribution will give exactly $\Lambda_1 = 2$
 366 because K'_1 is the mean, which in a symmetric distribution coincides with the median
 367 and thus yields $F(K'_{p_h}) = 1/2$. The exact value Λ_1 is easy to determine, as it is directly
 368 related to the mean, namely,

$$369 \quad \Lambda_1 := \frac{1}{1 - F(\mu)}, \quad (22)$$

370 while the exact value of Λ_∞ depends only on the tail index ξ of the distribution accord-
 371 ing to

$$372 \quad \Lambda_\infty = \begin{cases} \Gamma(1 - \xi)^{\frac{1}{\xi}} \\ e^\gamma \end{cases} \quad (23)$$

373 where $\gamma = 0.577$ is the Euler's constant.

374 Basing on the above estimates for Λ_1 and Λ_∞ the following approximation may be
 375 used for estimating Λ_{p_h} , which is satisfactory for several distributions:

$$376 \quad \Lambda_{p_h} \approx \Lambda_\infty + \frac{\Lambda_1 - \Lambda_\infty}{p_h}, \quad (24)$$

377 and, substituting in eq. (21)

$$378 \quad F(K'_{p_h}) \approx 1 - \frac{1}{\Lambda_\infty p_h + (\Lambda_1 - \Lambda_\infty)}. \quad (25)$$

379 Conversely, for a given non-exceedance probability F , we can calculate the quan-
 380 tile x as the K_{p_h} that corresponds to:

$$381 \quad p_h \approx \frac{1}{\Lambda_\infty(1-F)} + 1 - \frac{\Lambda_1}{\Lambda_\infty} \quad (26)$$

382 where, in our case, $F = 1 - \alpha/2$, being α the significance level of the confidence band.

383 For estimating Λ_1 an expression for the probability distribution of F is to be se-
 384 lected and plugged into eq. (22). Koutsoyiannis (2021) provides ready-to-use relation-
 385 ship for Λ_1 for several probability distributions. The distribution F can be assumed to
 386 be invariant over the range of the simulated river flows. Therefore, estimates for the tail
 387 index can be obtained by fitting the whole observed data sample (or the mean predic-
 388 tion sample obtained with the S-model) with a suitable probability distribution (we use
 389 the Pareto-Burr-Feller distribution for the case studies presented in Section 5). Note that
 390 the above distributional assumption on the whole data set has the only purpose of pro-
 391 viding estimates for the tail index ($F(\mu)$ is also required but this can readily be estimated
 392 from data even without fitting a distribution) and therefore we do not make any assump-
 393 tion on the distribution of each individual sample that is used for the estimation of the
 394 empirical quantiles at each time step.

395 4 Assessment of Goodness of Fit

396 Assessment of performance is essential to provide end users with an indication of
 397 the reliability of the S-model and its confidence limits. Besides providing values of the
 398 Pearson correlation coefficient between observed and simulated data and the Nash ef-
 399 ficiency for both the D-model and S-model, we also draw the diagnostic plots described
 400 below and report the percentage of observations lying outside the confidence limits, es-
 401 timated by using both order statistics and robust estimation.

402 4.1 Combined Probability-Probability (CPP) Plot

403 A simple graphical test is introduced here to assess the performances of the S-model.
 404 It is based on the comparison of the marginal distributions of observed and predicted
 405 variables. Here we refer to it as ‘‘Combined Probability-Probability’’ (CPP) plot. CPP
 406 is a plot of the empirical distribution function $F_w(w)$ of a stochastic variable \underline{w} against
 407 its value w . The variable is defined as the non-exceedance probability:

$$408 \quad \underline{w} := F_Q(q). \quad (27)$$

409 Its distribution function is $F_w(w) = P\{\underline{w} \leq w\} = P\{F_Q(q) \leq w\} = P\{q \leq F_Q^{-1}(w)\}$
 410 and hence:

$$411 \quad F_w(w) = F_q\left(F_Q^{-1}(w)\right). \quad (28)$$

412 In other words, $F_w(w)$ combines the distribution functions of predictions Q and real quan-
 413 tities q . The predictions are regarded as good if the plot $F_w(w)$ versus w is the equal-
 414 ity line, i.e., if $F_w(w) = w$, which means that the distribution of w is uniform. In this
 415 case $F_q^{-1}(w) = F_Q^{-1}(w)$. This is possible only if $F_Q(x)$ is identical to $F_q(x)$, which is
 416 what we would like to check. Note that a CPP plot lying above (below) the equality line
 417 indicates overprediction (underprediction) while a S-shaped CPP plot with the initial
 418 part above (below) the equality line and the second part below (above) the equality line
 419 indicates overestimation of low (high) flows and underestimation of high (low) flows.

420 In essence, the plot tests whether the two distributions, estimated from the data,
 421 are identical. We note that the CPP plot, except for assessing the proximity of the two
 422 marginal distributions, does not give any other indication if the predictions are good.

423 For example if \underline{Q} is completely independent from \underline{q} (as it may happen if an obviously ir-
 424 relevant model is used) but the two distributions are identical, again the distribution of
 425 w will be uniform.

426 4.2 Predictive Probability-Probability Plot

427 A second check is herein used to verify the reliability of the estimated confidence
 428 band. Laio and Tamea (2007) have introduced a diagnostic plot combining probability
 429 distributions of predictions and true values, which has become later popular in similar
 430 studies, having been termed “predictive quantile-quantile” (PQQ) plot (Eslamian, 2014),
 431 even though in the original paper it has been called simply probability plot. Here we re-
 432 fer to it as “predictive probability-probability” (PPP) plot because the plot actually rep-
 433 represents probabilities. PPP is a plot of the empirical distribution function $F_z(z)$, of a stochas-
 434 tic variable \underline{z} , where the latter also represents probability, i.e., a conditional non-exceedance
 435 probability, namely

$$436 \underline{z}_Q := F_{q|Q}(\underline{q}). \quad (29)$$

437 In other words, \underline{z} is the distribution function of the prediction evaluated for the observed
 438 value of the predictand. The idea of PPP comes from the Rosenblatt’s result that for
 439 any stochastic process \underline{x}_τ in discrete time $\tau = 1, 2, \dots$, the sequence of variables $\underline{z}_1, \underline{z}_2, \dots, \underline{z}_\tau$,
 440 whose values are:

$$441 z_\tau := P \{ \underline{x}_\tau \leq x_\tau | \underline{x}_{\tau-1} = x_{\tau-1}, \dots, \underline{x}_1 = x_1 \} = F_{x_\tau | x_{\tau-1}}(x_\tau | \mathbf{x}_{\tau-1}) \quad (30)$$

442 are independent and identically distributed with uniform distribution in $[0, 1]$. Note that
 443 here we used the vector notation $\mathbf{x}_{\tau-1} := [x_{\tau-1}, \dots, x_1]^T$ to represent all values of the
 444 process earlier than τ . One may see an analogy of \underline{z}_Q defined in eq. (29) with z_τ defined
 445 in (30) as they both are predictive distributions. Extending this analogy, one would ex-
 446 pect that different \underline{z} defined by eq. (29) would also be independent and identically dis-
 447 tributed, which allows considering the different values as a sample of a single variable
 448 \underline{z} . In turn, this enables estimating the distribution function of \underline{z} from the sample.

449 The information conveyed by the PPP plot is useful as it provides an overview of
 450 the reliability of the estimated confidence band for any confidence level, by showing de-
 451 partures of the calibrated predictive distribution from the optimal one. Specifically, a
 452 shape of the validation curve above or below the equality line indicates overprediction
 453 and underprediction, respectively, while a shape above (below) the equality line in the
 454 first part of the diagram and below (above) the same line in the second part means that
 455 the forecast is narrow (large). Figure 2 provides a graphical overview of the above fea-
 456 tures, while more details are given by Laio and Tamea (2007). Furthermore, the depar-
 457 ture of the PPP plot from the equality line is a relative (with respect to the sample size)
 458 measure of the number of points lying below the lower and above the upper confidence
 459 limit. For example, coverage probabilities for confidence level of 0.8 are related to seg-
 460 ments A and B in figure 2.

461 In fact, the percentage of observations lying below a confidence limit is such that
 462 for a given Q the probability that the true discharge is not greater than q is

$$463 P \{ \underline{q} \leq q | \underline{Q} = Q \} = F_{q|Q}(q). \quad (31)$$

464 If we choose a non-exceedance probability α , $0 \leq \alpha \leq 1$, so that, for any Q , $F_{q|Q}(q) =$
 465 α then the latter relationship specifies a confidence curve for q , which is a function $q =$
 466 $h(Q)$, given that α is constant. The probability

$$467 P \{ \underline{q} \leq h(Q) | \underline{Q} = Q \} = F_{q|Q}(h(Q)) = \alpha \quad (32)$$

468 is constant, independent of Q . Moreover, given the definition of z and its property not
 469 to depend on Q , one obtains $z = \alpha$. If the distribution of z is uniform in $(0,1)$, i.e. $F_z(z) =$

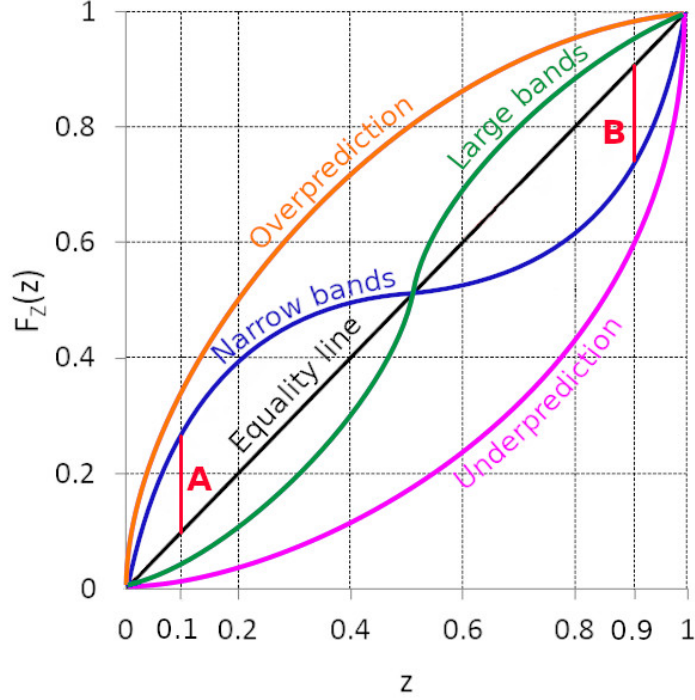


Figure 2. Information conveyed by the PPP plot.

470 z , the value of $F_z(z)$ at the point $z = \alpha$ will be equal to α . Therefore any deviation from
 471 uniformity is a relative measure of the number of observations exceeding the value α that
 472 would be expected that fall outside the confidence limit.

473 Note that the non-parametric fully data based approach of Bluecat infers $F_{q|Q}(q)$
 474 in calibration from eq. (16), basing on subranges of Q . Therefore, if one estimates the
 475 z_τ sample for the same values of Q the empirical distribution of z will be clearly uniform,
 476 regardless of the D-model performance or any other feature of the processes q_τ and Q_τ .
 477 Therefore, the PPP plot for the calibration period of Bluecat will always be a straight
 478 line (equality line) by definition, because the data to be predicted are those that have
 479 been used to estimate the predictive distribution.

480 5 Case Studies

481 Bluecat was first tested with control experiments that have been presented by Koutsoyiannis
 482 and Montanari (2020). These confirmed the capability of the method to estimate reli-
 483 ably stochastic predictions and coverage probabilities in controlled conditions.

484 Here we present two case studies to test the performances of Bluecat in real world
 485 applications. They refer to the cases of the Arno river at Subbiano and the Siver river
 486 at Fornacina, for which a rainfall-runoff model is used to elaborate river flow predictions.
 487 The Sieve river is a tributary of the Arno river. They flow in the Tuscany Region, in Italy.
 488 Figure 3 presents a schematic map of the river basins. Climate is continental with low
 489 flows during Summer and high flows in the Fall and Spring seasons. Occasionally high
 490 flow events may occur during the winter.

We apply to both case studies the rainfall-runoff model HyMod (Boyle, 2000; Montanari, 2005) with 5 parameters. These are C_m [length], the maximum storage capacity within the basin), β [dimensionless], the degree of spatial variability of the soil moisture capacity within the basin, α [dimensionless], a factor for partitioning the flow between two routing procedures, k_1 [time] and k_2 [time], characteristic times for the two routing components.

For both case studies we calibrated the HyMod model by minimizing the Nash-Sutcliffe efficiency. It is well known that performance metrics are affected by significant sampling uncertainty (Clark et al., 2021; Barber et al., 2020). Lamontagne et al. (2020) have shown that estimation robustness may be improved by performing a preliminary logarithmic transformation of observed and simulated river flow data. Therefore, we considered the following transformation, which can be applied also to intermittent river flows (Koutsogiannis, 2021):

$$y = \lambda \log\left(1 + \frac{x}{\lambda}\right) \quad (33)$$

where x and y are original and transformed data, respectively, and λ is a parameter. For $\lambda \rightarrow 0$ and $\lambda \rightarrow \infty$ eq. (33) becomes equivalent to the logarithmic and the identity ($y = x$) transform, respectively.

It is well known that a limited training for hydrologic models may cause overparameterisation, which in turn implies that model performances in calibration may not deliver a useful information on the reliability of model predictions in validation. This issue will be further discussed in Section 6.

We estimated confidence limits by applying both robust estimation and order statistics by adopting a confidence level of 80%. We selected $m_1 = m_2 = 100$ which means that each prediction distribution is estimated over a sample of $m_1 + m_2 + 1 = 201$ observations. For the extreme values of the prediction the sample size was reduced when enough lower/higher predictions were not available (see the note at the bottom of Section 3.1). The S-model predictions were obtained by estimating the median value of the conditional probability distribution given by eq. (4), although CPP plots were drawn for the mean stochastic prediction as well.

Median prediction and confidence band for the S-model were estimated for both the calibration and validation period. Of course we expect better performances of the S-model for the calibration period while the validation exercise is expected to provide an indication of the Bluecat performances for out of sample prediction. Goodness of fit is estimated by the performance indicators discussed in Section 4.

5.1 Arno River at Subbiano

The catchment of the Arno river at Subbiano is located within the mountain belt of the Northern Apennines, with mean, minimum and maximum elevation of 750, 250 and 1657 m above sea level, respectively. The catchment area is about 752 km² and the average catchment slope is about 14%. The data of mean areal daily rainfall (estimated from raingauge observations) and evapotranspiration (estimated from temperature data) span the 22-year period 1992-2013. We use the first 20 years for model calibration and the last two years for model validation. Optimization was performed after transforming data as in eq. (33) with $\lambda = 0.0001$, a value that was selected by looking at the S-model performances in calibration. Calibrated model parameters are given in Table 1. For the calibration period the Pearson correlation coefficient between the D-model outputs Q and the observed values q is 0.84, which means that the model is able to explain $0.84^2 = 71\%$ of the total variance. The Nash efficiency is 0.63.

Figure 4 shows the results of the application of Bluecat in calibration mode with robust estimation. In the left panel a scatterplot of D-model predictions versus observed values and S-model predictions is shown, along with the related confidence limits. The

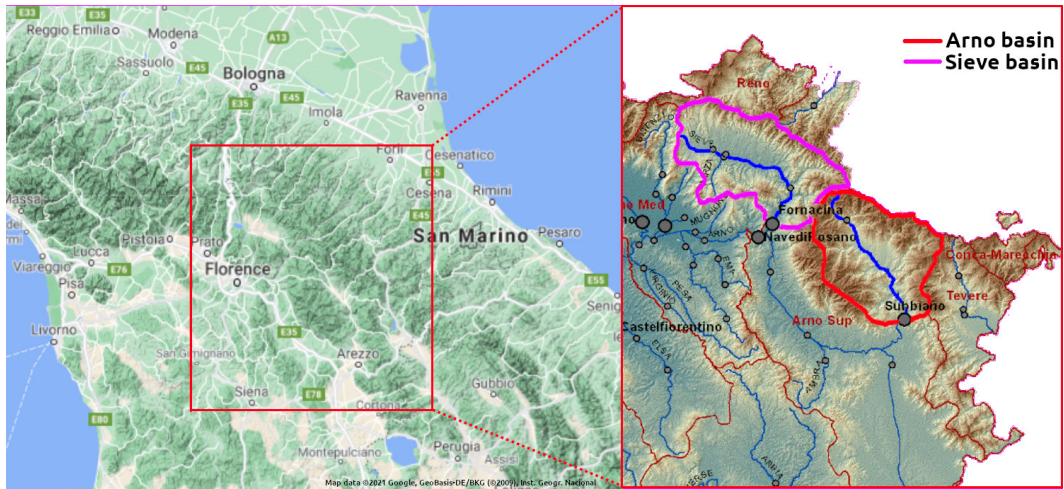


Figure 3. Basins of the Arno river at Subbiano and the Sieve river at Fornacina.

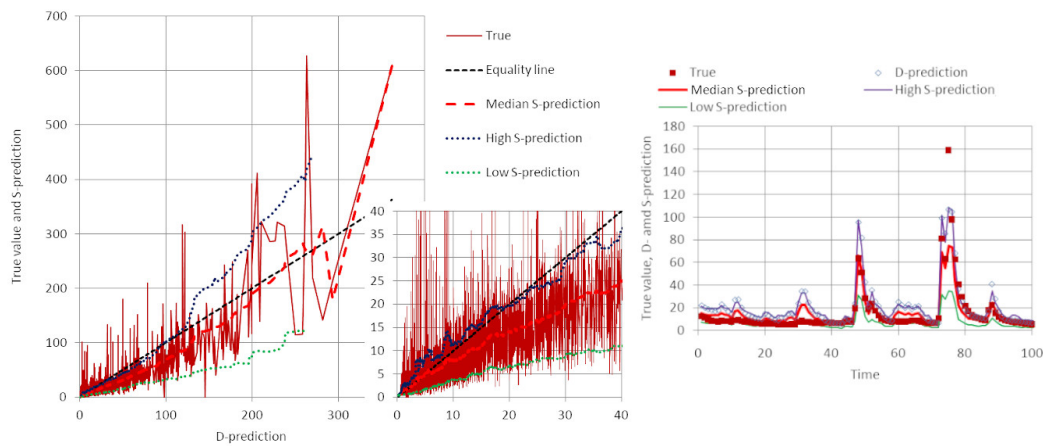


Figure 4. D-model and S-model predictions, along with confidence limits, for the calibration period of the Arno river at Subbiano. The right panel depicts 100 days of the calibration period, where the first day is January 1st, 2011.

541 inset shows a detailed representation of the low flow range. The right panel depicts 100
 542 days of the calibration period, where the first day is January 1st, 2011.

543 The S-model displayed improved predicting performances, with a Pearson correla-
 544 tion coefficient of 0.88 and a Nash efficiency of 0.77 (median prediction). Figure 4, par-
 545 ticularly in the inset, also shows that the D-model overpredicts low discharges and un-
 546 derpredicts high ones. The bias is reduced by the S-model. Coverage probabilities are
 547 reported in Table 2, for confidence band estimated with both order statistics and robust
 548 estimation. The CPP plot, shown in Figure 6, confirms the prediction bias of the D-model
 549 and the improved performances of the S-model which, however, still overpredicts the low
 550 flows as Figure 4 anticipated.

551 The results of the validation are shown in Figure 5, Table 2 and Figure 6. The right
 552 panel in Figure 5 depicts 100 days of the validation period, where the first day is Jan-
 553 uary 1st, 2013. The D-model performance in validation is summarised by a Pearson cor-

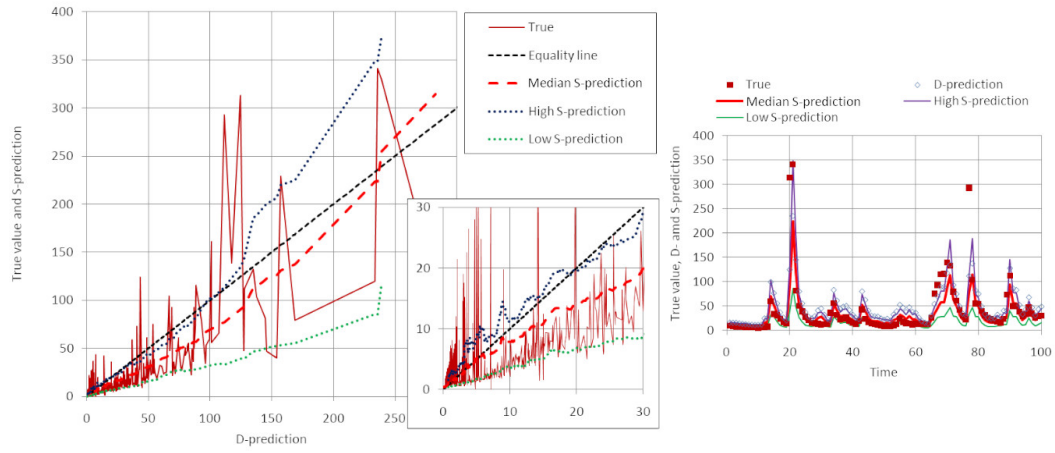


Figure 5. D-model and S-model predictions, along with confidence limits, for the validation period of the Arno river at Subbiano. The right panel depicts 100 days of the validation period, where the first day is January 1st, 2013.

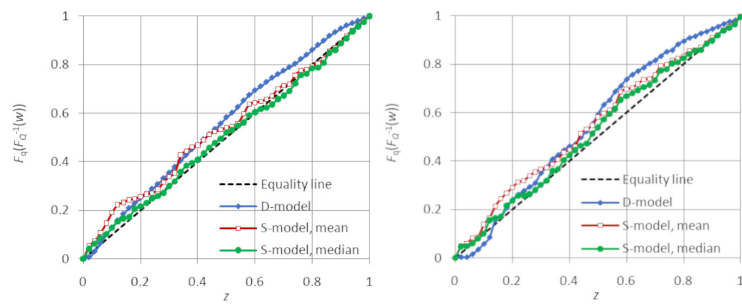


Figure 6. Combined probability-probability (CPP) plots for the predictions of the river flows of the Arno river at Subbiano in calibration (left) and validation (right).

Table 1. HyMod model calibrated parameters for the considered case studies

Basin	$C_m[mm]$	$\beta[-]$	$\alpha[-]$	$k_1[days]$	$k_2[days]$
Arno	336	0.10	0.61	24.34	1.25
Sieve	323	0.20	0.55	4.61	357.53

554 relation coefficient of 0.80 and a Nash efficiency of 0.57. Slightly better performances are
 555 given by the S-model prediction, with Pearson coefficient of 0.81 and a Nash efficiency
 556 of 0.62. The CPP plot confirms that the S-model improves the performances in terms
 557 of probability distribution of the predictions and proves the slightly better performances
 558 of the median with respect to the mean of the probability distribution given by eq. (4)
 559 to compute the S-model prediction. It also suggests an overestimation and underestima-
 560 tion of low and high flows, respectively.

561 The PPP plot is reported in Figure 10 (left) and shows that in validation the confi-
 562 dence limits are narrow. This outcome is confirmed by the percentage of observations
 563 lying outside the confidence limits, which are reported in Table 2, which are higher than
 564 the values of 10% for each band that one would expect for a confidence level of 80%. Fur-
 565 ther consideration on the PPP plot results for the Arno River are found in the Section
 566 6.

567 5.2 Sieve River at Fornacina

568 The Sieve river is a tributary of the Arno river that is also located in the North-
 569 ern Apennines, with mean, minimum and maximum elevation of 488, 96 and 1637 m above
 570 sea level, respectively. The catchment area is about 846 km² and the average catchment
 571 slope is about 12%. The data of mean areal hourly rainfall (estimated from raingauge
 572 observations) and evapotranspiration (estimated from temperature observations) span
 573 the 5-year period 1992-1996. The flow regime of the Sieve river is intermittent with the
 574 presence of about 4% of zero values in the available record.

575 We use the data from June 1st, 1992 to December 31st, 1994 for model calibra-
 576 tion and the data from June 2nd, 1995 to December 31st, 1996 for model validation. Note
 577 that we discarded the January-May period for both calibration and validation because
 578 high flows typically occur in that season that are not satisfactorily reproduced by Hy-
 579 Mod for the limited duration of the model warm up. We maximized the Nash-Sutcliffe
 580 efficiency to calibrate the parameters without applying any transformation to the data,
 581 as this led to the best S-model performances in terms of median prediction and cover-
 582 age probabilities.

583 Calibrated model parameters are given in Table 1. For the calibration period the
 584 correlation coefficient between the D-model outputs Q and the observed values q is 0.91,
 585 which means that the model is able to explain 82% of the total variance. The Nash ef-
 586 ficiency is 0.81. Figure 7 confirms the good fit of the model in calibration. The right panel
 587 depicts 150 hours of the calibration period starting from September 16th, 1992 at 5 AM.

588 The calibration results confirm the improved performances of the S-model, whose
 589 mean prediction has a Pearson correlation coefficient of 0.94 and Nash efficiency of 0.88.
 590 Figure 7, particularly in the inset, shows that the S-model corrects the prediction bias
 591 of the D-model. The percentage of points lying above and below the confidence limits
 592 is reported in Table 2. The CPP plot, shown in Figure 9, confirms the improved perfor-
 593 mances of the S-model and in particular its effectiveness in correcting the D-model bias
 594 in the high flow domain.

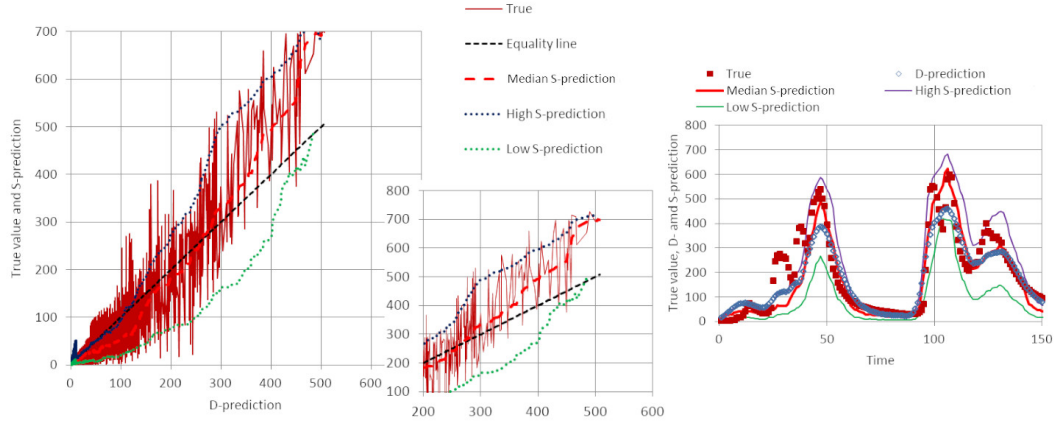


Figure 7. D-model and S-model predictions, along with confidence limits, for the calibration period of the Sieve river at Fornacina. The right panel depicts 150 hours of the calibration period starting from September 16th, 1992 at 5 AM.

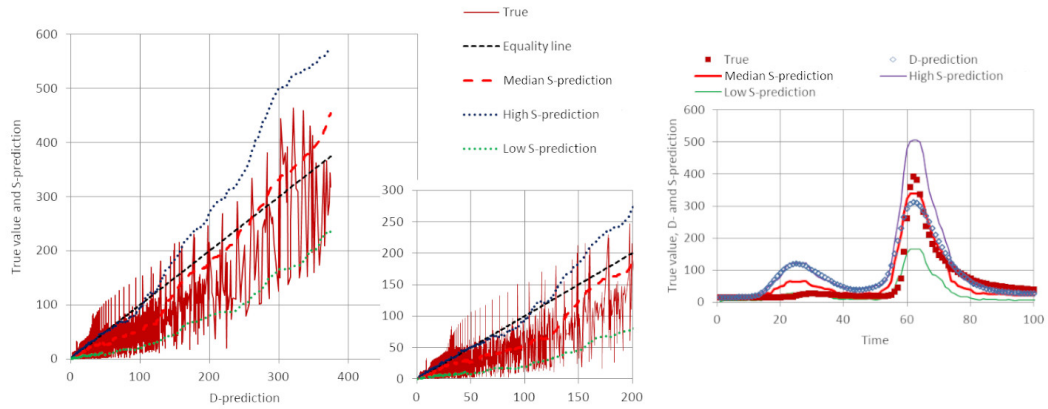


Figure 8. D-model and S-model predictions, along with confidence limits, for the validation period of the Sieve river at Fornacina. The right panel depicts 150 hours of the validation period starting from January 5th, 1996.

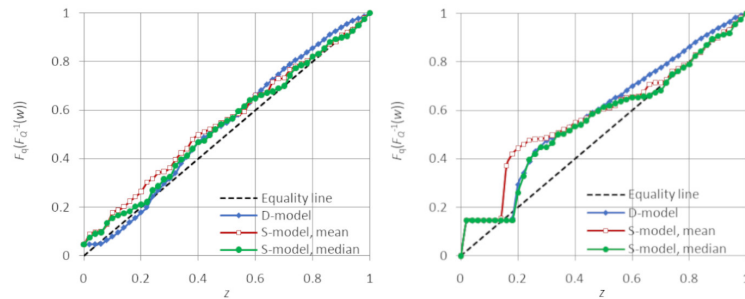


Figure 9. Combined probability-probability (CPP) plots for the predictions of the river flows of the Sieve river at Fornacina in calibration (left) and validation (right).

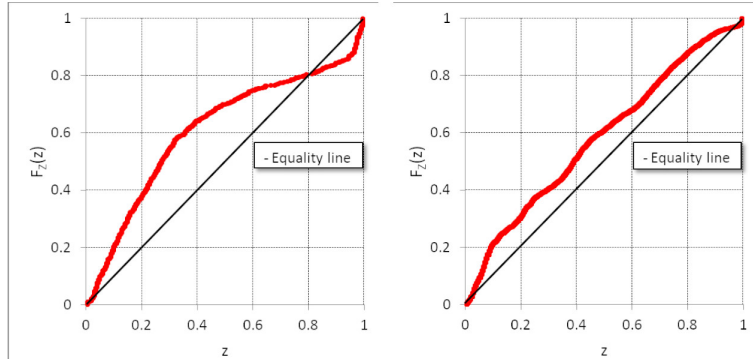


Figure 10. Predictive probability-probability (PPP) plots for the validation of the river flows predictions for the Arno river (left) and the Sieve river (right).

Table 2. Percentage of observations lying outside the 80% confidence limits for the considered case studies. Band was estimated with both order statistics and robust estimation. Subscripts h and l refer to upper and lower limit, respectively.

Arno calibration		Arno validation		Sieve calibration		Sieve validation	
$\%_h$	$\%_l$	$\%_h$	$\%_l$	$\%_h$	$\%_l$	$\%_h$	$\%_l$
Robust estimation							
10%	8%	17%	16%	17%	7%	13%	14%
Estimation with order statistics							
9%	10%	17%	22%	8%	9%	6%	16%

595 Validation results are shown in Figure 8, where the right panel depicts 150 hours
 596 of the validation period starting from January 5th, 1996 at 12 AM, and Figure 9. The
 597 D-model performance in validation is summarized by a Pearson correlation coefficient
 598 of 0.87 and a Nash efficiency of 0.53. The low value of the Nash efficiency is due to the
 599 significant overestimation of the low flows by the D-model. It is interesting to note that
 600 the S-model prediction exhibits a better fit with a Pearson coefficient of 0.88 and a Nash
 601 efficiency of 0.66. The latter is markedly improved thanks to the capability of Bluecat
 602 to correct the prediction bias. As for the confidence band, the PPP plot shows overall
 603 a good fit with a slight overprediction especially with regard to the lower limit (see also
 604 Table 2).

605 The results of the two case studies will be further discussed in Section 6.

606 6 Discussion

607 In introducing Bluecat we assumed that the probability distribution of the observed
 608 data, conditioned to the D-model simulation, can be reliably inferred from a calibration
 609 exercise (see Sections 2 and 3). Actually, this assumption holds asymptotically, namely,
 610 when the size of the calibration data sample is large. Furthermore, the assumption that
 611 we made that input and parameter uncertainty are satisfactorily resembled by the prob-
 612 ability distribution given by eq. (4) also holds asymptotically.

613 When the calibration data set is not extended enough one may experience over-
 614 parameterisation, which implies that the calibrated model exhibits satisfactory perfor-

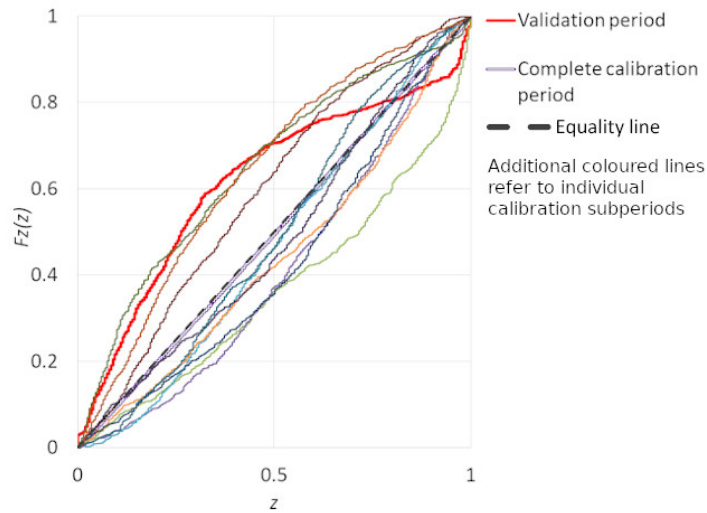


Figure 11. Sampling variability for the PPP plot of the Arno river in calibration and comparison with the PPP plot in validation.

615 mances in calibration that are not confirmed in validation. Therefore, in such cases the
 616 D-model errors in calibration may be much smaller than those in validation, which im-
 617 plies that the S-model generated by Bluecat may underestimate prediction uncertainty.
 618 That is, confidence band may be narrow, which means that the PPP plot would be S-
 619 shaped with the first and second part displaced above and below the equality line, re-
 620 spectively.

621 Furthermore, a limited extension of the validation period may imply uncertainty
 622 due to sampling variability. Namely, even if the confidence limits are statistically cor-
 623 rect they may still provide a poor assessment of uncertainty when referring to specific
 624 and short prediction periods.

625 To inspect this issue, we performed an additional experiment for the Arno river by
 626 referring to the calibration period. We first computed the PPP plot in calibration, there-
 627 fore obtaining an equality line as expected (see figure 11). Then, we redrew the PPP plot
 628 for 10 non-overlapping subperiods including 731 observations, which is precisely the length
 629 of the validation period. As expected, figure 11 shows that sampling variability causes
 630 a dispersion of the obtained PPP plots. For the sake of comparison, figure 11 also shows
 631 the PPP plot for the validation period, which is almost entirely included within the en-
 632 velop of the calibration PPP plots obtained for the same sample size. Therefore, figure
 633 11 shows that the deviation from the equality line that we obtained for the Arno river
 634 in validation may be explained by sampling variability.

635 About the CPP plot, one should always take into account that the marginal dis-
 636 tributions of predicted and observed data may be incidentally similar even if the predic-
 637 tion is poor. In particular, this may happen when the model performances in terms of
 638 correlation and Nash efficiency are far from satisfactory.

639 Regarding the case studies presented here it is interesting to note that for both Arno
 640 and Sieve rivers the stochastic prediction outperformed the deterministic model by cor-
 641 recting its bias for the various flow regimes. This outcome confirms that the additional
 642 value provided by the S-model is technically useful.

643 With regard to the confidence band, for the cases presented here, we indeed found
 644 that the observations lying outside the higher and lower confidence limits in validation

645 are often higher than the value of 10% for each band that one would expect for a con-
646 fidence level of 80% (see Table 2). Such deviations are expected when the simulation
647 period is short, even due merely to sampling variability, as illustrated with the Arno river
648 case study.

649 In technical applications it is important for the user to recognize the cases of “huge
650 uncertainty in uncertainty assessment”. First, we conclude that an accurate selection of
651 the model calibration period is particularly important for Bluecat, which is calibrated
652 at each local flow range. It is not possible to provide a general rule for assessing if a cal-
653 ibration period is long enough, as the answer depends on the type of model, the vari-
654 ability of the modeled processes, data seasonality and many others. It may be useful to
655 split the available data sample in non-overlapping pieces and perform repeated valida-
656 tion tests to assess whether model performances are stable. The split sample exercise
657 also allows to infer sampling variability. Second, we suggest that the final model train-
658 ing before application is carried out by using the largest possible data set and paying
659 particular attention to detect possible model deficiencies that may not be resembled by
660 the estimated conditional probability distribution of eq. (4).

661 We would like to discuss further the assumption of stationarity, which may be re-
662 garded as a limitation if one believes that the impact due to a possibly changing climate
663 may be better predicted with a non-stationary approach (for an extended discussion on
664 this subject see, e.g., Luke et al. (2017) and Montanari and Koutsoyiannis (2014a)). We
665 also note that the conditional distribution given by eq. (4) might be seasonal, although
666 part of the seasonality features are already incorporated in the D-model (for example,
667 a large prediction of discharge would appear during the rainy, rather than the dry, pe-
668 riod). There are many possible solutions for applying Bluecat in a non-stationary con-
669 text. We may suggest to first consider a D-model with time varying (perhaps seasonal)
670 parameters under the assumption that the uncertainty of the non-stationary model is
671 described by a stationary distribution as given by eq. (4). If one would like to consider
672 a non-stationary uncertainty, then a parametric and non-stationary distribution (per-
673 haps a Pareto-Burr-Feller distribution with time varying seasonal parameters) may be
674 adopted to describe uncertainty as described in Section 3.1, by paying particular atten-
675 tion to the increased risk of overparameterization that non-stationary models imply. In-
676 deed, exploring the above dependencies in a stochastic framework would require an ex-
677 tended calibration data set to compensate the uncertainty introduced by additional model
678 complexity. Overall, such modelling choices will unavoidably increase uncertainty and
679 therefore would hardly be advisable for copying with real-world problems. If the extent
680 of the data set is large enough, in cases justifying a seasonal approach, partitioning the
681 whole data set into seasons is a possible solution to ensure that both the D-model and
682 Bluecat provide a good fit of seasonality. If a permanent change of the process statis-
683 tics is detected (e.g. due to urbanization) it would be recommendable to “stationarize” the
684 data, adapting them to the current conditions and perform similar adaptations to the
685 D-model. This is similar (albeit opposite) to “naturalization” of data series that is typ-
686 ically made in cases of river modifications due to dams and so forth.

687 One may wonder what is the distinguishing behavior of Bluecat with respect to the
688 approaches that we previously proposed (Montanari & Koutsoyiannis, 2012; Sikorska et
689 al., 2015). We first note that Bluecat relies on different assumptions and procedures. In
690 Montanari and Koutsoyiannis (2012) we adopted a meta-Gaussian distribution to de-
691 scribe uncertainty of model predictions which were preliminarily transformed to stabi-
692 lize their variance. Bluecat, in a similar manner as Sikorska et al. (2015)), avoids data
693 transformation as the conditional probability distribution is automatically defined by the
694 data. Furthermore, in Montanari and Koutsoyiannis (2012) and Sikorska et al. (2015)
695 we accounted for parameter uncertainty at the expense of a more demanding approach
696 for model calibration and application, which is a concern as in a data assimilation con-
697 text calibration is to be frequently repeated. In fact, by avoiding any data transforma-

698 tion and offering a fast calibration, Bluecat allows technical applications with limited com-
699 putational requirements and time.

700 Bluecat indeed shares some similarities with the nearest neighbouring method by
701 Sikorska et al. (2015), which may be also used to correct the D-model bias (see, for in-
702 stance, Ehlers et al. (2019)). However, we note that Bluecat infers the conditional prob-
703 ability distribution of the true data, while Sikorska et al. (2015) estimate the conditional
704 probability distribution of the simulation error. Thus, they estimate the prediction un-
705 certainty of the D-model rather than updating the D-model to the S-model. Therefore
706 Bluecat provides a more comprehensive perspective. In view of the above differences, the
707 user may select the most appropriate approach for the considered case study, with the
708 awareness that model selection should be tailored to the underlying assumptions and op-
709 erational needs.

710 Although Bluecat has been conceived to be applied to one single model, a multi-
711 model application would be straightforward. It was already mentioned in Section 3 that
712 an extension where Q is a vector containing the current and earlier predictions by the
713 D-model is possible, yet here we study the simpler scalar version of the model. Likewise,
714 the multi-model case is another possible vector version of Bluecat, where the vector Q
715 contains the outcomes of the various D-models.

716 We believe that the application of Bluecat to the considered case studies offers en-
717 couraging performances for technical applications. Indeed, Bluecat does, under a rigor-
718 ous statistical interpretation and clear assumptions, what the intuition of a technician
719 would suggest: to correct model predictions and estimate their uncertainty by looking
720 at model performances in the simulation of known data. It is a straightforward and ex-
721 tremely simple concept.

722 Finally, the end users should be informed that hydrologic modeling, including un-
723 certainty assessment, is always uncertain and therefore the information provided by the
724 confidence band should be interpreted critically. Nevertheless, this information is tremen-
725 dously useful: by selecting an appropriate confidence level Bluecat provides the desired
726 information for an assigned safety level of the prediction.

727 **7 The Bluecat package**

728 In order to facilitate the application of Bluecat we make available a software work-
729 ing under the R-environment (R Core Team, 2013) to fit the HyMod rainfall-runoff model
730 and estimate its prediction uncertainty. Model fitting can be performed by maximizing
731 the Nash-Sutcliffe efficiency using either untransformed data or transformed with equa-
732 tion (33), with the option of selecting two different optimization algorithms. Confidence
733 limits can be defined by estimating empirical quantiles through order statistics or robust
734 estimation (see Section 3.1 and 3.2). Assessment of the goodness of fit is performed by
735 plotting the CPP and PPP plots and estimating the Nash-Sutcliffe efficiency. The soft-
736 ware is accompanied by instructions (to be displayed with the R help function) and data
737 bases of rainfall and potential evapotranspiration for the Arno and Sieve case studies that
738 have been presented here. We also include instructions to be used within R to reproduce
739 the case studies and the results we presented above.

740 While the package focuses on river flow prediction with HyMod, it can be easily
741 adapted by substituting HyMod with any deterministic model. In fact, the model rou-
742 tine is isolated into a subroutine, currently written in the Fortran 95 programming lan-
743 guage, that can be quickly replaced.

744 The software is available for download at the web address:
745 <https://github.com/albertomontanari/hymodbluecat>
746 along with instructions to compile it in R.

8 Conclusions

We introduce here a new method identified with the acronym “Bluecat” for simulating and predicting hydrologic processes, which is based on the use of a generic deterministic model that is subsequently converted to a stochastic formulation. The latter provides an update of the deterministic prediction along with uncertainty assessment with a transparent data based approach.

The results of the presented case studies confirm the distinguishing features of Bluecat, its reliability and robustness. In fact, for both case studies the stochastic version of the deterministic model provided an improvement of the performances of the deterministic model alone, both in calibration and validation. Furthermore, the estimated confidence band turned out to be informative: even if some uncertainty affected the estimation of coverage probabilities, we provided quantitative tests to verify their reliability. In fact, for both case studies Bluecat improved the prediction and provided confidence limits with an innovative and rigorous information content for technical applications.

In our opinion, for its computational efficiency and transparency Bluecat is a step forward for hydrologic modeling with uncertainty assessment. It is also flexible, as it can work in conjunction with any type of deterministic model and can be extended to multimodel applications or multiple predictor variables.

In view of technical applications, particular care is to be paid to the reliability and extension of the calibration data set. In fact, it is usual in hydrology to work in poorly gauged conditions, which may lead to overparametrisation, sampling variability and consequent inflation of uncertainty. Although Bluecat has been proven to be robust, the reliability of the deterministic model calibration should be carefully considered in order to avoid a “huge uncertainty in uncertainty assessment”. We discussed potential solutions to support operational assessment of calibration reliability, which should ultimately rely on a careful assessment by end users.

When developing Bluecat and preparing this paper we decided to give high priority to simplicity, transparency, openness and reproducibility. For this reason we make available a software to support Bluecat operational applications and reproduction of the case studies presented here. We are looking forward to interacting with users for improving the software in an open access and open source context.

Acknowledgments

Preparation of this paper was slowed down by the outbreak of COVID19, which took all of the working time of AM for managing the emergency. We would like to address a special thought to those who suffered and lost their lives from the pandemic, with the hope that their sacrifice may help humanity to more effectively recognize that life and health are first priorities.

The software that has been used to develop this work, a package working under the R environment, is open source and available for download at:
<https://github.com/albertomontanari/hymodbluecat>.
We thank Emanuele Baratti and Elena Toth who helped to collect the data that were used for developing the case studies, which are included into the above software, along with instruction to reproduce the results presented here.

We are grateful to Richard Vogel, John Quilty, an anonymous reviewer and an anonymous Associate Editor for their encouraging and constructive comments, which greatly helped us to improve the paper. We are also thankful to Keith Beven and Alberto Viglione for providing very useful suggestions.

References

- 795
- 796 Barber, C., Lamontagne, J. R., & Vogel, R. M. (2020). Improved estimators of
797 correlation and r^2 for skewed hydrologic data. *Hydrological Sciences Journal*,
798 *65*(1), 87–101.
- 799 Beven, K. (2006). A manifesto for the equifinality thesis. *Journal of hydrology*,
800 *320*(1-2), 18–36. doi: 10.1016/j.jhydrol.2005.07.007
- 801 Beven, K. (2009). Comment on “equifinality of formal (dream) and informal
802 (glue) bayesian approaches in hydrologic modeling?” by jasper a.
803 vrugt, cajo jf ter braak, hoshin v. gupta and bruce a. robinson. *Stochas-
804 tic environmental research and risk assessment*, *23*(7), 1059–1060. doi:
805 10.1007/s00477-008-0283-x
- 806 Beven, K., & Binley, A. (1992). The future of distributed models: model calibration
807 and uncertainty prediction. *Hydrological processes*, *6*(3), 279–298. doi: 10
808 .1002/hyp.3360060305
- 809 Beven, K., & Lane, S. (2019). Invalidation of models and fitness-for-purpose: a rejec-
810 tionist approach. In *Computer simulation validation* (pp. 145–171). Springer.
- 811 Blöschl, G. (2008). Flood warning-on the value of local information. *International
812 Journal of River Basin Management*, *6*(1), 41–50. doi: 10.1080/15715124.2008
813 .9635336
- 814 Blöschl, G., Bloschl, G., Sivapalan, M., Wagener, T., Savenije, H., & Viglione, A.
815 (2013). *Runoff prediction in ungauged basins: synthesis across processes, places
816 and scales*. Cambridge University Press.
- 817 Boyle, D. (2000). *Multicriteria calibration of hydrological models* (Unpublished doc-
818 toral dissertation). Univ of Arizona, Tucson.
- 819 Bulygina, N., & Gupta, H. (2009). Estimating the uncertain mathematical structure
820 of a water balance model via bayesian data assimilation. *Water Resources Re-
821 search*, *45*(12). doi: 0.1029/2007WR006749
- 822 Clark, M. P., Vogel, R. M., Lamontagne, J. R., Mizukami, N., Knoben, W. J.,
823 Tang, G., ... others (2021). The abuse of popular performance metrics
824 in hydrologic modeling. *Water Resources Research*, e2020WR029001. doi:
825 10.1029/2020WR029001
- 826 Ehlers, L., Wani, O., Koch, J., Sonnenborg, T., & Refsgaard, J. (2019). Using a
827 simple post-processor to predict residual uncertainty for multiple hydrological
828 model outputs. *Advances in Water Resources*, *129*, 16–30.
- 829 Eslamian, S. (2014). *Handbook of engineering hydrology: modeling, climate change,
830 and variability*. CRC Press.
- 831 Frame, J., Kratzert, F., Klotz, D., Gauch, M., Shelev, G., Gilon, O., ... Nearing,
832 G. S. (2021). Deep learning rainfall-runoff predictions of extreme events. *Hy-
833 drology and Earth System Sciences Discussions*. doi: 10.5194/hess-2021-423
- 834 Kavetski, D., Fenicia, F., Reichert, P., & Albert, C. (2018). Signature-domain
835 calibration of hydrological models using approximate bayesian computation:
836 Theory and comparison to existing applications. *Water Resources Research*,
837 *54*(6), 4059–4083.
- 838 Koutsoyiannis, D. (2019). Knowable moments for high-order stochastic character-
839 ization and modelling of hydrological processes. *Hydrological sciences journal*,
840 *64*(1), 19–33. doi: 10.1080/02626667.2018.1556794
- 841 Koutsoyiannis, D. (2021). *Stochastics of hydroclimatic extremes – a cool look at risk*.
842 Hellenic Academic Ebooks. Retrieved from [http://hdl.handle.net/11419/
843 6522](http://hdl.handle.net/11419/6522)
- 844 Koutsoyiannis, D., & Montanari, A. (2015). Negligent killing of scientific concepts:
845 the stationarity case. *Hydrological Sciences Journal*, *60*(7-8), 1174–1183. doi:
846 10.1080/02626667.2014.959959
- 847 Koutsoyiannis, D., & Montanari, A. (2020). A brisk local uncertainty estimator for
848 hydrologic simulations and predictions (blue cat). In *Egu general assembly con-
849 ference abstracts* (p. 10125). doi: 10.5194/egusphere-egu2020-10125

- 850 Krzysztofowicz, R. (1999). Bayesian theory of probabilistic forecasting via determin-
851 istic hydrologic model. *Water Resources Research*, *35*(9), 2739–2750. doi: 10
852 .1029/1999WR900099
- 853 Laio, F., & Tamea, S. (2007). Verification tools for probabilistic forecasts of continu-
854 ous hydrological variables. *Hydrology and Earth System Sciences*, *11*(4), 1267–
855 1277. doi: 10.5194/hess-11-1267-2007
- 856 Lamontagne, J. R., Barber, C. A., & Vogel, R. M. (2020). Improved estimators of
857 model performance efficiency for skewed hydrologic data. *Water Resources Re-*
858 *search*, *56*(9), e2020WR027101.
- 859 Luke, A., Vrugt, J. A., AghaKouchak, A., Matthew, R., & Sanders, B. F. (2017).
860 Predicting nonstationary flood frequencies: Evidence supports an updated
861 stationarity thesis in the u nited s tates. *Water Resources Research*, *53*(7),
862 5469–5494. doi: 10.1002/2016WR019676
- 863 Montanari, A. (2005). Large sample behaviors of the generalized likelihood uncertain-
864 tainty estimation (glue) in assessing the uncertainty of rainfall-runoff simula-
865 tions. *Water resources research*, *41*(8).
- 866 Montanari, A. (2011). Uncertainty of hydrological predictions. In P. Wilderer (Ed.),
867 *Treatise on water science, vol. 2* (p. 459-478). Elsevier.
- 868 Montanari, A., & Brath, A. (2004). A stochastic approach for assessing the uncertain-
869 tainty of rainfall-runoff simulations. *Water Resources Research*, *40*(1). doi: 10
870 .1029/2003WR002540
- 871 Montanari, A., & Grossi, G. (2008). Estimating the uncertainty of hydrological fore-
872 casts: A statistical approach. *Water Resources Research*, *44*(12). doi: 10.1029/
873 2008WR006897
- 874 Montanari, A., & Koutsoyiannis, D. (2012). A blueprint for process-based modeling
875 of uncertain hydrological systems. *Water Resources Research*, *48*(9). doi: 10
876 .1029/2011WR011412
- 877 Montanari, A., & Koutsoyiannis, D. (2014a). Modeling and mitigating natural haz-
878 ards: Stationarity is immortal! *Water resources research*, *50*(12), 9748–9756.
879 doi: 10.1002/2014WR016092
- 880 Montanari, A., & Koutsoyiannis, D. (2014b). Reply to comment by grey nearing
881 on “a blueprint for process-based modeling of uncertain hydrological systems”.
882 *Water Resour. Res.*, *50*, 6264–6268. doi: 10.1002/2013WR014987
- 883 Nearing, G. S. (2014). Comment on “a blueprint for process-based modeling of un-
884 certain hydrological systems” by alberto montanari and demetris kousoyiannis.
885 *Water Resources Research*, *50*, 6260–6263. doi: 10.1002/2013WR014812
- 886 Pagano, T. C., Wood, A. W., Ramos, M.-H., Cloke, H. L., Pappenberger, F., Clark,
887 M. P., ... others (2014). Challenges of operational river forecasting. *Journal*
888 *of Hydrometeorology*, *15*(4), 1692–1707. doi: 10.1175/JHM-D-13-0188.1
- 889 Papacharalampous, G., Tyralis, H., & Koutsoyiannis, D. (2019). Comparison of
890 stochastic and machine learning methods for multi-step ahead forecasting of
891 hydrological processes. *Stochastic Environmental Research and Risk Assess-*
892 *ment*, *33*(2), 481–514. doi: 10.1007/978-3-540-79881-1{-}3
- 893 Papacharalampous, G., Tyralis, H., Koutsoyiannis, D., & Montanari, A. (2020).
894 Quantification of predictive uncertainty in hydrological modelling by har-
895 nassing the wisdom of the crowd: A large-sample experiment at monthly
896 timescale. *Advances in Water Resources*, *136*, 103470. doi: 10.1016/
897 j.advwatres.2019.103470
- 898 Papacharalampous, G., Tyralis, H., Langousis, A., Jayawardena, A. W., Sivakumar,
899 B., Mamassis, N., ... Koutsoyiannis, D. (2019a). Large-scale comparison of
900 machine learning regression algorithms for probabilistic hydrological modelling
901 via post-processing of point predictions. In *Geophysical research abstracts*
902 (Vol. 21). doi: 10.1007/s00521-020-05172-3
- 903 Papacharalampous, G., Tyralis, H., Langousis, A., Jayawardena, A. W., Sivakumar,
904 B., Mamassis, N., ... Koutsoyiannis, D. (2019b). Probabilistic hydrological

- 905 post-processing at scale: Why and how to apply machine-learning quantile
 906 regression algorithms. *Water*, *11*(10), 2126. doi: 10.3390/w11102126
- 907 Quilty, J., & Adamowski, J. (2020). A stochastic wavelet-based data-driven frame-
 908 work for forecasting uncertain multiscale hydrological and water resources
 909 processes. *Environmental Modelling & Software*, *130*, 104718.
- 910 R Core Team. (2013). R: A language and environment for statistical computing
 911 [Computer software manual]. Vienna, Austria. Retrieved from [http://www.R-](http://www.R-project.org/)
 912 [project.org/](http://www.R-project.org/)
- 913 Ramos, M. H., Van Andel, S. J., & Pappenberger, F. (2013). Do probabilistic fore-
 914 casts lead to better decisions? *Hydrology and Earth System Sciences*, *17*(6),
 915 2219–2232. doi: 10.5194/hess-17-2219-2013,2013
- 916 Reggiani, P., Todini, E., Boyko, O., & Buizza, R. (2021). Assessing uncertainty for
 917 decision-making in climate adaptation and risk mitigation. *International Jour-*
 918 *nal of Climatology*, *41*(5), 2891–2912. doi: 10.1002/joc.6996
- 919 Schoups, G., & Vrugt, J. A. (2010). A formal likelihood function for parameter
 920 and predictive inference of hydrologic models with correlated, heteroscedas-
 921 tic, and non-gaussian errors. *Water Resources Research*, *46*(10). doi:
 922 10.1029/2009WR008933
- 923 Sikorska, A. E., Montanari, A., & Koutsoyiannis, D. (2015). Estimating the
 924 uncertainty of hydrological predictions through data-driven resampling
 925 techniques. *Journal of Hydrologic Engineering*, *20*(1), A4014009. doi:
 926 10.1061/(ASCE)HE.1943-5584.0000926
- 927 Spear, R., & Hornberger, G. (1980). Eutrophication in peel inlet—ii. identification
 928 of critical uncertainties via generalized sensitivity analysis. *Water research*,
 929 *14*(1), 43–49. doi: 10.1016/0043-1354(80)90040-8
- 930 Tajiki, M., Schoups, G., Hendricks Franssen, H., Najafinejad, A., & Bahremand,
 931 A. (2020). Recursive bayesian estimation of conceptual rainfall-runoff model
 932 errors in real-time prediction of streamflow. *Water Resources Research*, *56*(2),
 933 e2019WR025237. doi: 10.1029/2019WR025237
- 934 Tyrallis, H., Papacharalampous, G., Burnetas, A., & Langousis, A. (2019). Hy-
 935 drological post-processing using stacked generalization of quantile regression
 936 algorithms: Large-scale application over conus. *Journal of Hydrology*, *577*,
 937 123957. doi: 10.1016/j.jhydrol.2019.123957
- 938 Tyrallis, H., Papacharalampous, G., & Langousis, A. (2019). A brief review of ran-
 939 dom forests for water scientists and practitioners and their recent history in
 940 water resources. *Water*, *11*(5), 910. doi: 10.3390/w11050910
- 941 Valdez, E. S., Anctil, F., & Ramos, M.-H. (2021). Choosing between post-processing
 942 precipitation forecasts or chaining several uncertainty quantification tools in
 943 hydrological forecasting systems. *Hydrology and Earth System Sciences Discus-*
 944 *sions*, 1–40. doi: 10.5194/hess-2021-391
- 945 Vrugt, J. A., Ter Braak, C. J., Gupta, H. V., & Robinson, B. A. (2009). Equifinal-
 946 ity of formal (dream) and informal (glue) bayesian approaches in hydrologic
 947 modeling? *Stochastic environmental research and risk assessment*, *23*(7),
 948 1011–1026. doi: 10.1007/s00477-008-0274-y